

Suppression of surface barriers in superconductors by columnar defects

A. E. Koshelev and V. M. Vinokur

Materials Science Division, Argonne National Laboratory, Argonne, Illinois 60439

(Received 24 April 2001; revised manuscript received 14 June 2001; published 12 September 2001)

We investigate the influence of columnar defects in layered superconductors on the thermally activated penetration of pancake vortices through the surface barrier. Columnar defects, located near the surface, facilitate penetration of vortices through the surface barrier, by creating “weak spots,” through which pancakes can penetrate into the superconductor. Penetration of a pancake mediated by an isolated column, located near the surface, is a two-stage process involving hopping from the surface to the column and the detachment from the column into the bulk; each stage is controlled by its own activation barrier. The resulting effective energy is equal to the maximum of those two barriers. For a given external field there exists an optimum location of the column for which the barriers for the both processes are equal and the reduction of the effective penetration barrier is maximal. At high fields the effective penetration field is approximately 2 times smaller than in unirradiated samples. We also estimate the suppression of the effective penetration field by column clusters. This mechanism provides further reduction of the penetration field at low temperatures.

DOI: 10.1103/PhysRevB.64.134518

PACS number(s): 74.60.Ge

I. INTRODUCTION

The properties of the Abrikosov vortex state of type-II superconductors with artificially manufactured columnar defects have attracted a great deal of current attention. Motivated originally by a technological quest for enhanced vortex pinning, superconductors with columnar defects revealed a vast diversity of remarkable phenomena. The possibility to introduce controlled disorder and to tune parameters (such as vortex density and interactions between vortices) has made them one of the favorite experimental systems for studies of the statistical mechanics and dynamics of a glassy state (see the recent review in Ref. 1 and references therein).

On the other hand, the magnetic response of high-temperature superconductors is known to be controlled to a large extent by the creep of vortices over the Bean-Livingston surface barrier,²⁻⁶ an important manifestation of which is the exponential temperature dependence of the effective penetration field. It was recently observed that columnar defects can strongly facilitate the creep of pancake vortices over the surface barrier and reduce the penetration field.⁷ Usually pinning by disorder and surface barriers are considered to be competing effects that alternatively control the magnetic response in the vortex state. In this paper we consider an interplay between surface and bulk pinning and develop a theory for the disorder-assisted surface creep in highly anisotropic superconductors, focusing on the case of randomly distributed columnar defects. This effect is somewhat analogous to the tunneling of quantum particles in the presence of subbarrier disorder.⁸

It is clear from a general consideration that surface imperfections create weak spots, facilitating the penetration of vortices through the Bean-Livingston barrier. However, a quantitative theory for imperfections of an arbitrary kind is not available. Special kinds of surface irregularities have been considered in Refs. 9–11. We address well-defined surface disorder created by controlled irradiation with heavy ions. In this case vortices enter the sample near the weak spots where columnar defects are located close enough to the surface to

suppress the surface barrier. Vortex penetration consists of two steps (see Fig. 1): (i) the capturing of the vortex onto a near-surface column and (ii) the detachment of the trapped vortex into the bulk. The resulting effective barrier for pancake penetration via an isolated column is the maximal value of the two barriers corresponding to the above processes. The capturing process has, in its turn, a two-channel character and may occur either via the direct motion of a pancake to a column or via the nucleation of an *antivortex* at the column and its subsequent advance towards the surface (see Fig. 1). The capturing process is controlled by the channel with the *smallest* barrier. If the mediating column is located far from the surface, the penetration process is controlled by the transfer of a vortex from the surface to this column. When the column is sufficiently close to the surface, the controlling barrier corresponds to detaching a vortex from the column to the bulk. For every external field there exists an optimal location of the column for which the reduction of the barrier is maximal, and penetration of pancakes into the sample occurs mainly via such optimally placed columns.

One can expect that the surface barrier may be suppressed even more efficiently in very rare places where several columns happen to be near the surface. The net contribution to the penetration rate from such events is determined as a balance between their small probability and the strong local suppression of the barrier. We estimate in Sec. III the collective suppression by the column clusters. At low temperatures the collective suppression always becomes more efficient than the single-column mechanism.

II. VORTEX ENERGY NEAR SURFACE IN THE PRESENCE OF AN ISOLATED COLUMNAR DEFECT

We consider an irradiated superconductor with insulating columnar defects oriented along the c axis in an external magnetic field also applied along the c axis. Let an isolated columnar defect have radius R and be located at a distance L from the surface of superconductor (see Fig. 2). The energy of a pancake vortex located between the surface and column

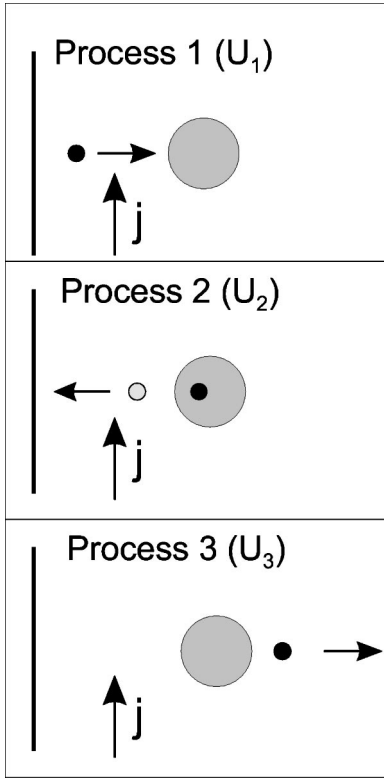


FIG. 1. Mechanisms of penetration of the pancake vortex from the surface into the bulk of a superconductor: (a) Nucleation of the vortex at the column via the motion of vortex from the surface, (b) nucleation of the vortex at the column via motion of an antivortex from the column to the surface, and (c) motion of the vortex from the column into the bulk.

at distance x from the surface consists of two parts: the direct interactions with the column and the surface, $U_{int}(x)$, and the interaction with the Meissner current, $U_j(x)$. We introduce dimensionless variables measuring length in units of R , energy in units of $s\varepsilon_0 \equiv s\Phi_0^2/(4\pi\lambda)^2$, current in units of $c\Phi_0/(4\pi\lambda)^2R$, and magnetic field in units of $\Phi_0/4\pi\lambda R$. Here λ is the in-plane London penetration depth and s is the

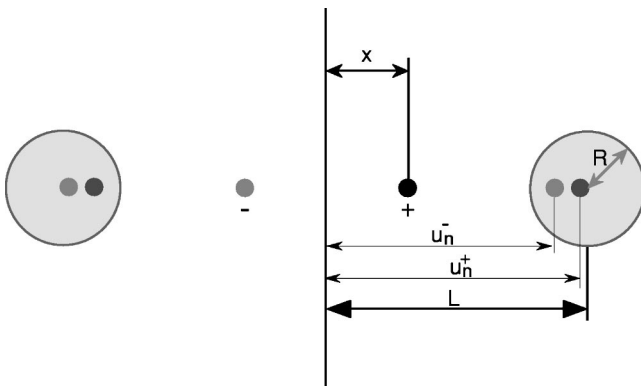


FIG. 2. Geometry: a pancake vortex between the surface and a columnar defect. Interaction with the surface and the column can be described in terms of an infinite set of positive and negative images obtained by multiple subsequent reflections by the surface and the column (only the first two images inside the column are shown).

interlayer spacing. We also use the notation $l \equiv L/R$.

A. Direct interaction with surface and column

The interaction of the vortex with either the plain surface or an isolated column can be calculated by virtue of the image technique.¹² The interaction with the surface is obtained by placing a negative vortex at the point $-x$ and the interaction with the isolated column can be obtained by placing a negative vortex at point $l-1/(l-x)$ inside the column and a positive vortex at the column center.¹³ In the case where the vortex is confined between the column cavity and the surface, adding these images only would not solve the problem because the currents due to the surface image do not satisfy the boundary conditions at the surface of the columnar cavity and vice versa. To compensate the currents of the surface image, one has to add its image (reflection) inside the column. This eliminates the vortex in the column center and adds a vortex at the point $l-1/(l+x)$. After that we have to add the surface image of this vortex at the point $-l+1/(l+x)$. Continuing these reflections, we obtain an infinite set of positive and negative images. We label coordinates of the positive (negative) images inside the column after the n th double reflection as u_n^+ (u_n^-) [every such image has a corresponding surface image of opposite sign at $-u_n^+$ ($-u_n^-$)]. The $(n+1)$ st image is obtained by reflecting the n th image with respect to the surface and then reflecting it again with respect to the column. This yields the following recurrence relations:

$$u_{n+1}^- = l - \frac{1}{l + u_n^-}, \quad u_{n+1}^+ = l - \frac{1}{l + u_n^+}, \quad (1)$$

with

$$u_1^- = l - \frac{1}{l-x}, \quad u_1^+ = l - \frac{1}{l+x},$$

As follows from Eqs. (1), both the negative and positive images approach the same limiting position $u_\infty = \sqrt{l^2 - 1}$ as $n \rightarrow \infty$. The interaction energy is then expressed as an infinite series in the coordinates of all images:

$$U_{int}(x) = \ln \frac{1.47R}{\xi} + \ln 2x + \sum_{n=1}^{\infty} \ln \left| \frac{(u_n^- - x)(u_n^+ + x)}{(u_n^- + x)(u_n^+ - x)} \right|. \quad (2)$$

Note that this expression is valid for a vortex located at either side of the column, i.e., for both $0 < x < l-1$ and $x > l+1$. The supercurrent distribution around the column containing the trapped vortex coincides with the distribution corresponding to a vortex placed at the point $\sqrt{l^2 - 1}$ and its surface image. The energy of this state is given by

$$U_{tr}(l) = \ln(l + \sqrt{l^2 - 1}).$$

The energy, corresponding to an antivortex at the point x , which controls the competing process of antivortex motion from the column to the surface, is obtained analogously and reads

$$U_{int}^{(av)}(x) = U_{int}(x) + 2 \ln \frac{\sqrt{l^2-1}-x}{\sqrt{l^2-1}+x} + \ln(l + \sqrt{l^2-1}). \quad (3)$$

Here the second term on the right-hand side (RHS) describes the interaction of the antivortex with the trapped vortex while the third term gives the self-energy of the trapped vortex.

To solve the recurrence relations (1), we introduce a new variable f_n for both the positive and negative images $u_n \equiv u_n^\pm$ as

$$f_n = -\frac{\sqrt{l^2-1} + u_n}{\sqrt{l^2-1} - u_n}$$

and transform Eq. (1) into a simple relation

$$f_{n+1} = a^2 f_n,$$

with $a = l + \sqrt{l^2-1} > 1$, which can be easily solved: $f_n = a^{2n} f_1$. This allows us to obtain closed analytical formulas for the image coordinates:

$$u_n^+ = \sinh b \frac{x + \tanh(nb) \sinh b}{\tanh(nb)x + \sinh b},$$

$$u_n^- = \sinh b \frac{x - \tanh(nb) \sinh b}{\tanh(nb)x - \sinh b}, \quad (4)$$

with $b \equiv \ln(l + \sqrt{l^2-1})$ and $l = \cosh b$. Taken together, Eqs. (2) and (4) solve the problem of finding the energy of a vortex located on the perpendicular to the surface passing through the center of the column. This result can also be obtained using a complex plane representation and the conformal mapping

$$w = \ln \left[\frac{\sqrt{l^2-1} + z}{\sqrt{l^2-1} - z} \right].$$

It transforms the semispace $x > 0$ with a circular hole at $z = (l, 0)$ into the rectangular area $\{0 < w_1 < b, -\pi < w_2 < \pi\}$ with periodical boundary condition along the w_2 direction.

B. Interaction with the Meissner currents

A column (cylindrical cavity) placed near the surface disturbs the pattern of the screening supercurrent induced by the external magnetic field and changes accordingly the contribution to the vortex energy arising from surface screening current. The current $\mathbf{j}(\mathbf{r})$ has to satisfy $\text{div} \mathbf{j} = 0$. This means that it can be expressed in terms of a supercurrent potential $\phi_j(\mathbf{r})$ as

$$j_y = -\frac{\partial \phi_j}{\partial x}, \quad j_x = \frac{\partial \phi_j}{\partial y}.$$

We consider the situation where all relevant distances are smaller than the London penetration depth so that we can neglect screening effects and assume $\text{curl} \mathbf{j} = 0$, which implies that the potential satisfies the Laplace equation $\Delta \phi_j = 0$. The

problem of finding the current distribution is thus equivalent to the problem of the polarization of a metallic cylinder near a metallic surface by the external electric field parallel to the surface.¹⁵ Since the normal components of \mathbf{j} should vanish at the surface *and* at the column, both the external boundary of the superconductor and the boundary of the column should be equipotential surfaces. Setting $\phi_j(0, y) = 0$, we define $\phi_j(\mathbf{r})$ as the interaction energy of a vortex at the point \mathbf{r} with the Meissner current. Note that at large distances from the column, the x component of the current should vanish; thus, far from the column, $\mathbf{j} = (0, j)$ with $j = cH/(4\pi\lambda)$. The current distribution near an isolated cylinder can be obtained by putting vortex dipole $(j, 0)$ at the center of the cylinder; this dipole induces potential

$$\phi_j = -jx \left(1 - \frac{1}{(x-L)^2 + y^2} \right).$$

To satisfy the boundary condition at the surface one has to add surface image of this dipole, i.e., to put dipole $(-j, 0)$ at $x = -L$. However, the currents of this surface image do not satisfy the boundary conditions for the column and we again have to add the column image of the surface image. Continuing this process, we again obtain an infinite set of dipole images inside the column. Note that this sequential reflection in the column does not preserve the magnitude of a dipole. Reflecting pair of opposite vortices located near the point $(x, 0)$, we derive that the magnitude of column reflection of dipole is smaller by factor of $1/(l-x)^2$ than the magnitude of the original dipole. Denoting the coordinate of the dipole resulting from the n double reflections as x_n and its magnitude as $j p_n$, we derive the recurrence relations

$$p_{n+1} = \frac{1}{(l+x_n)^2} p_n, \quad x_{n+1} = l - \frac{1}{l+x_n}, \quad (5)$$

with $x_1 = l$, $p_1 = 1$. Analytical solutions to these equations are given by

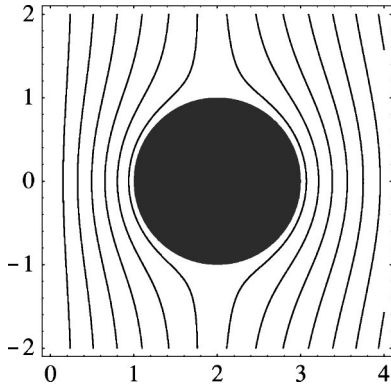
$$x_n = \sqrt{l^2-1} \coth nb,$$

$$p_n = \frac{l^2-1}{\sinh^2 nb}, \quad (6)$$

where, again, $b \equiv \ln(l + \sqrt{l^2-1})$. The potential can be represented as an infinite series

$$\phi_j(\mathbf{r}) = -jx + j \sum_{n=1}^{\infty} \left[\frac{(x-x_n)p_n}{(x-x_n)^2 + y^2} + \frac{(x+x_n)p_n}{(x+x_n)^2 + y^2} \right].$$

The interaction energy of the vortex, located at the line $y = 0$, with the Meissner current is given by


 FIG. 3. Example of the current distribution for $l=2$.

$$\phi_j(x) \equiv \phi_j(x,0) = -jx + 2xj \sum_{n=1}^{\infty} \frac{P_n}{x^2 - x_n^2}.$$

Figure 3 illustrates the current distribution for $l=2$. When column is located sufficiently close to the surface, $l \rightarrow 1$, the current at the surface diverges as $j_y(0,0) = \sqrt{2}j/\sqrt{l-1}$, while the current at the opposite side of the column approaches a universal value,

$$j_y(l+1,0) \rightarrow j \left(1 + 2 \sum_{n=1}^{\infty} \frac{4n^2+1}{(4n^2-1)^2} \right) = (\pi^2/4)j \approx 2.47j.$$

The vortex–Meissner-current interaction energy becomes $\phi_j(l-1) = -j\sqrt{l^2-1}$ when the vortex is trapped by the column, and the total energy of the trapped vortex reads

$$U_{tr}(l,j) = \ln(l + \sqrt{l^2-1}) - j\sqrt{l^2-1}.$$

C. Activation barriers

As we have already mentioned, the penetration of a pancake into an irradiated superconductor happens in two steps: hopping from the surface to a column and detachment from the column into the bulk. The resulting effective barrier is equal to the maximum of the two barriers for the two processes. In addition, the nucleation of a vortex at the column (the first step) can occur via two channels: (i) as motion of a vortex from the surface to a column or (ii) by nucleation at and the subsequent motion of an *antivortex* from the column to the surface. The effective barrier for this first step is, thus, the smaller one: the process goes through the easier channel. For every fixed position of the column there exists a certain value $j_{cd}(l)$ of the surface current, above which the state with the one flux quantum trapped in the column becomes energetically favorable:

$$j_{cd}(l) = \frac{\ln(l + \sqrt{l^2-1})}{\sqrt{l^2-1}}.$$

This current is plotted in Fig. 4. The magnetic field corresponding to this current is given by

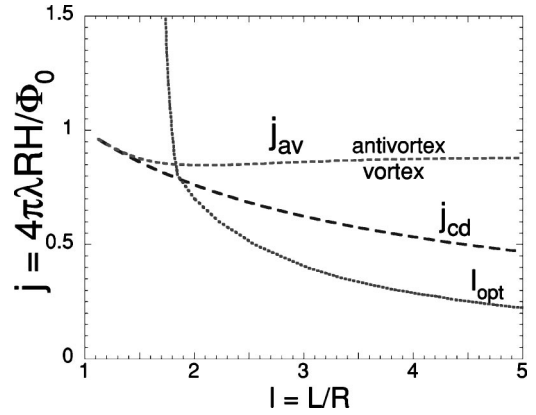


FIG. 4. Lines in the j - l plane at which the penetration mechanism changes: at currents $j > j_{cd}(l)$ it is energetically favorable to put one flux quantum on the column; at currents $j > j_{av}(l)$ nucleation of the flux quantum at the column occurs by motion of an antivortex from the column to the surface. The line $l_{opt}(j)$ gives the optimum position of the column corresponding to the maximum suppression of the barrier.

$$H_{cd}(L) = \frac{\Phi_0}{4\pi\lambda\sqrt{L^2-R^2}} \ln \left(\frac{L + \sqrt{L^2-R^2}}{R} \right).$$

Using the total energy of the vortex located at the point $(x,0)$,

$$U_v(x) = U_{int}(x) + \phi_j(x),$$

one can calculate the activation barrier for the vortex to hop from a surface to the column (process 1 in Fig. 1):

$$\mathcal{U}_1(l,j,R/\xi) = \max_{0 < x < l-1} U_v(x).$$

Analogously, making use of the expression for the energy of the couple, the antivortex at the point $(x,0)$ and the vortex inside the column,

$$U_{av}(x) = U_{int}^{(av)}(x) - \phi_j(x) - j\sqrt{l^2-1},$$

one obtains the barrier for the motion of the antivortex from the column to the surface (process 2 in Fig. 1):

$$\mathcal{U}_2(l,j,R/\xi) = \max_{0 < x < l-1} U_{av}(x).$$

The trajectory of the process, i.e., the channel that will actually govern vortex penetration, depends on the magnitude of the applied current. At small currents the surface-to-column process dominates while at sufficiently large currents the vortex-antivortex mechanism comes into play. The characteristic current $j_{av}(l)$ separating these two regimes depends on the position of the column and is determined by the solution of the equation $\mathcal{U}_1(l,j_{av}) = \mathcal{U}_2(l,j_{av})$. The plot of $j_{av}(l)$ is shown in Fig. 4 together with $j_{cd}(l)$. The barrier to activate the vortex from the column into the bulk of superconductor (process 3 in Fig. 1) is given by

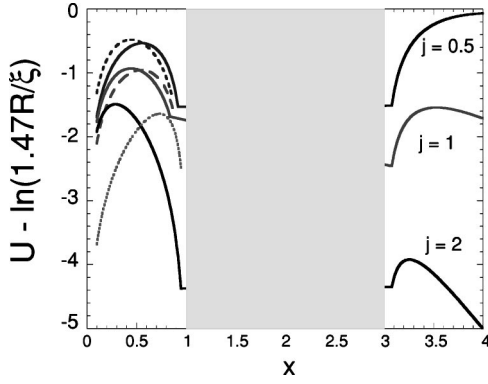


FIG. 5. The evolution of the energy profiles with increasing screening surface current j for $l=2$. On the left-hand side, solid lines represent the energy profiles $U_v(x)$ for the vortex moving from the surface to the column, and dashed lines represent the energy profiles for an antivortex, $U_{av}(x)$, moving in the opposite direction.

$$\mathcal{U}_3(l, j, R/\xi) = \begin{cases} \max_{x>l+1} [U_v(x)], & j < j_{cd}(l), \\ \max_{x>l+1} [U_v(x)] - U_{tr}(l, j), & j > j_{cd}(l). \end{cases}$$

Finally, the total barrier corresponding the channel surface \rightarrow column \rightarrow bulk reads

$$\mathcal{U}(l, j, R/\xi) = \max[\min(\mathcal{U}_1, \mathcal{U}_2), \mathcal{U}_3]. \quad (7)$$

In the following we will calculate the effective reduction of the surface barrier by the column

$$\delta\mathcal{U}(l, j) = \mathcal{U}(l, j, R/\xi) - \mathcal{U}_0(j, R/\xi), \quad (8)$$

which does not depend on the ratio R/ξ . Here

$$\mathcal{U}_0(j, R/\xi) = \ln \frac{1.47R}{\xi} + \ln \frac{2}{j} - 1 \quad (9)$$

is the barrier for pancake penetration through an ideal surface.^{2,4,6,16}

We will now turn to a numerical evaluation of the barriers. Figure 5 illustrates the evolution of the energy profiles $U_v(x)$ and $U_{av}(x)$ with increasing current for $l=2$. As one can see, at small current the position of the maximum energy is located on the right-hand side of the column while at large current it is located between the surface and column. Figure 6 shows examples of the l dependence of the column-induced barrier changes $\delta\mathcal{U}_1(l, j)$, $\delta\mathcal{U}_2(l, j)$, and $\delta\mathcal{U}_3(l, j)$ for different j . The barriers $\mathcal{U}_1(l, j)$ and $\mathcal{U}_2(l, j)$ are rapidly suppressed when the column approaches the surface, mainly because of the divergence of the surface current. On the other hand, the barrier $\delta\mathcal{U}_3(l, j)$ increases slowly with the decrease of l . Thus, for large l the total barrier is determined by $\mathcal{U}_1(l, j)$ [or $\mathcal{U}_2(l, j)$] and for small l it is determined by $\mathcal{U}_3(l, j)$. Figure 7 shows the l dependence of the total barrier $\mathcal{U}(l, j)$ for different l . For every value of the surface current (external field) there is an optimum location of the column l_{opt} for which suppression of the barrier is maximum. It cor-

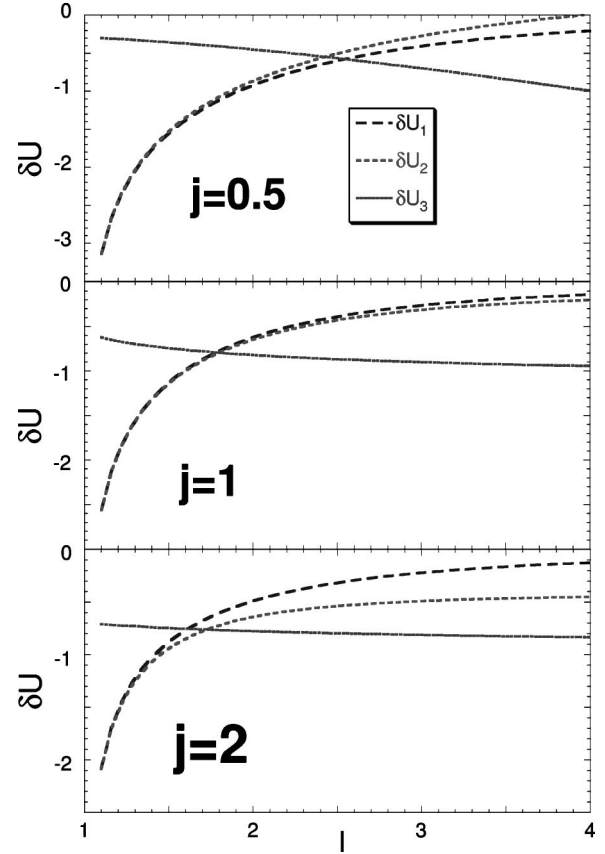


FIG. 6. Dependence of the energy barriers on the relative distance from the surface $l=L/R$ for the three processes shown in Fig. 1 for several values of j .

responds to a transition between the two mechanisms of penetration, i.e., $\mathcal{U}_3(l_{opt}, j) = \min(\mathcal{U}_1(l_{opt}, j), \mathcal{U}_2(l_{opt}, j))$. The line $l_{opt}(j)$ is shown at Fig. 4 together with $j_{cd}(l)$ and $j_{av}(l)$. Fig. 8 shows the current dependence of the barrier suppression for an optimally located column $\delta\mathcal{U}_{opt}(j) \equiv \delta\mathcal{U}(l_{opt}, j)$. This plot represents the main result of the paper. The important feature of this dependence is that at high currents it saturates at ≈ -0.76 .

An important manifestation of the surface barrier in high- T_c superconductors is the enhancement of the effective pen-

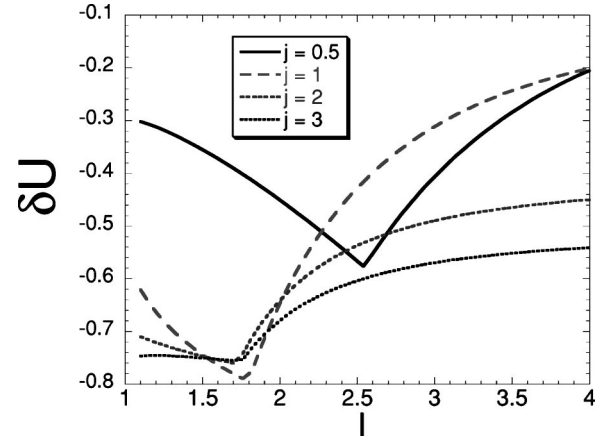


FIG. 7. l dependence of the total barrier for penetration from the surface into the bulk for several values of j .

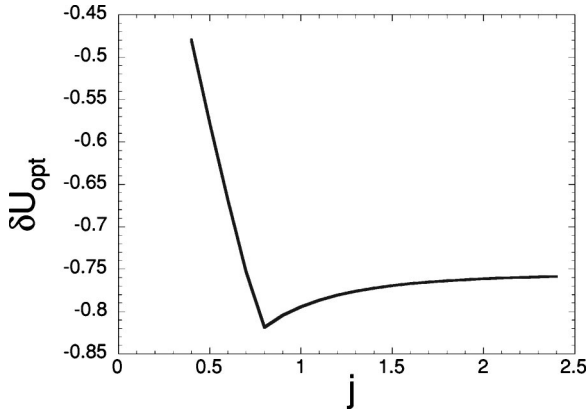


FIG. 8. j dependence of the energy barrier reduction for penetration of a vortex from the surface into the bulk for the *optimum* column location, i.e., for the minimum positions of $\delta U(l, j)$ plotted in Fig. 7. One can expect that this plot determines the reduction of the surface barrier in real irradiated samples in the single-column regime.

etration field.² When the penetration field is limited by thermal penetration through the surface barrier, the effective penetration field is determined by the equation $\mathcal{U}_0(H_{p0}) = CT$, where the numerical constant $C \approx 20-40$ is determined by the experimental time scale and by the attempt frequency.^{2,6} This gives the exponential temperature dependence of the penetration field. In irradiated samples the penetration field is expected to be shifted to a lower value, which is determined by $\mathcal{U}_0(H_p) + \delta\mathcal{U}(H_p) = CT$. In the field range $H_p \gg \Phi_0/4\pi\lambda R$ where the barrier reduction approaches the constant value $-0.76s\varepsilon_0$ we arrive at the very simple result $H_p \approx 0.47H_{p0}$.

III. COLLECTIVE SUPPRESSION OF THE SURFACE BARRIER BY COLUMN CLUSTERS

In the previous sections we considered suppression of the surface barrier due to an isolated columnar defect near the surface. Such a mechanism does not give the full picture. The barrier may be suppressed even more substantially in a small number of places where several columns occur to be close to the surface. The resulting enhancement of the average penetration rate comes as a trade between the suppression of the barrier and small probability of such event. In this section we estimate the contribution to the penetration rate and the reduction of the effective penetration field caused by clusters of defects. The optimal gate for the vortex entry will appear as several columns line up next to each other, forming thus a cut thrusting the sample normal to the surface. The width of the cut is $2R$ and its length is $2NR$, where N is the number of columns in such a cluster (see Fig. 9). In order to find the entry energy due to such a cluster we will follow Refs. 9 and 10, where the current and field distributions near the edge of the wedge-like surface crack were calculated. Consider thus a cut normal to the surface made of a chain of N columns. According to Refs. 9 and 10 the current near the tip of a thin crack grows as $j\sqrt{2NR/x}$ when the distance x from the tip of the crack (the last column) falls into the

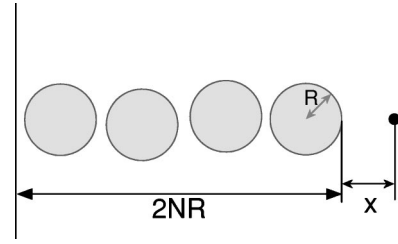


FIG. 9. The gate at the surface created by an improbable event when N columns form a chain. Such gates dominate flux penetration at low temperatures.

interval $R < x \ll 2NR$ and saturates at $j\sqrt{2N}$ for $x \leq R$. Here j is the Meissner current far away from the crack. The suppression of the barrier depends on the relation between the position of the energy maximum x_0 and R .

Consider the case $x_0 > R$ first. Making use of the results of Refs. 9 and 10, we write the energy of vortex at distance x from the tip of the crack as¹⁷

$$E(x) = -\frac{s\Phi_0}{c} j\sqrt{2NRx} + s\varepsilon_0 \ln \frac{x}{\xi}.$$

Accordingly, the barrier for this gate configuration [the maximum value of $E(x)$] is

$$\mathcal{U} = \mathcal{U}_0 - s\varepsilon_0 \ln \frac{\Phi_0 j NR}{c\varepsilon_0}, \quad (10)$$

where the bare barrier \mathcal{U}_0 in real units is given $\mathcal{U}_0 = s\varepsilon_0 \ln(j_{dp}/j)$ and j_{dp} is the depairing current. The energy $E(x)$ achieves its maximum value at the point $x_0 = 2(c\varepsilon_0/\Phi_0 j)^2/(NR)$, which has to satisfy the conditions $R < x_0 < NR$.

In order to estimate the effective penetration rate one has to determine the size of the clusters giving maximal contribution to vortex entry. The probability to find a chain of N columns in a row scales as $(\pi R^2 n_d)^N$ with n_d being the column concentration. Therefore the contribution from such chains to the penetration rate is given by

$$\begin{aligned} & \sum_N (\pi R^2 n_d)^N \exp\left(\frac{s\varepsilon_0}{T} \ln \frac{\Phi_0 j NR}{c\varepsilon_0}\right) \\ &= \sum_N \exp\left(-N \ln \frac{1}{\pi R^2 n_d} + \frac{s\varepsilon_0}{T} \ln \frac{\Phi_0 j NR}{c\varepsilon_0}\right), \end{aligned} \quad (11)$$

and becomes maximal at the optimal N :

$$N = \frac{s\varepsilon_0}{T \ln(1/\pi R^2 n_d)} > \max\left[1, \frac{2c\varepsilon_0}{\Phi_0 j R}\right].$$

Now the condition $x_0 > R$ reduces to

$$T > \frac{s\varepsilon_0}{\ln(1/\pi R^2 n_d)} \left(\frac{\Phi_0 j R}{2c\varepsilon_0}\right)^2.$$

In this “high-temperature” regime the change of the surface barrier is

$$\begin{aligned}\delta\mathcal{U} &\approx -s\varepsilon_0 \ln \frac{s\Phi_0 j R}{2cT \ln(1/\pi R^2 n_d)} \\ &= -s\varepsilon_0 \ln \frac{sR\Phi_0 H}{8\pi\lambda T \ln(1/\pi R^2 n_d)},\end{aligned}$$

where, again, $j = cH/4\pi\lambda$.

The effective penetration barrier is determined by the relation

$$s\varepsilon_0 \ln \frac{H_c H_T}{H^2} = CT, \quad (12)$$

with $H_T = sR\Phi_0/8\pi\lambda T \ln(1/\pi R^2 n_d)$, which gives

$$H_p = \sqrt{H_c H_T} \exp\left(-\frac{CT}{2s\varepsilon_0}\right). \quad (13)$$

Consider now the regime $x_0 < R$, corresponding to low temperatures. In this case the energy of the vortex is given by

$$E(x) = -\frac{s\Phi_0}{c} j \sqrt{2N} x + s\varepsilon_0 \ln \frac{x}{\xi}.$$

The position of the energy maximum and the barrier are given by

$$x_0 = \frac{c\varepsilon_0}{\Phi_0 j \sqrt{2N}},$$

$$U = s\varepsilon_0 \ln \frac{c\varepsilon_0}{\Phi_0 \xi j \sqrt{2N}} \approx U_0 - \frac{s\varepsilon_0}{2} \ln N.$$

Following the same route one arrives at the optimal cluster length as

$$N = \frac{s\varepsilon_0}{2T \ln(1/\pi R^2 n_d)} > 1,$$

and, accordingly, the change of the barrier is

$$\delta U = -\frac{s\varepsilon_0}{2} \ln \frac{s\varepsilon_0}{2T \ln(1/\pi R^2 n_d)}.$$

Contrary to the case of individual columns, the cluster gate exhibits the temperature dependence: the depression of the barrier *decreases* logarithmically with growing temperature. The change of the effective penetration field is determined by

$$s\varepsilon_0 \ln \frac{H_c}{H_p} - \frac{s\varepsilon_0}{2} \ln \frac{s\varepsilon_0}{2T \ln(1/\pi R^2 n_d)} = CT$$

or

$$H_p = \sqrt{\frac{2T \ln(1/\pi R^2 n_d)}{s\varepsilon_0}} H_{p0}. \quad (14)$$

This formula gives the effective penetration fields at low temperatures. It is probably more relevant to the experimental situation than the “high-temperature” result (13). We see that long clusters of columnar defects forming the cracklike configurations further (as compared to the effect of an individual column) suppress the surface barrier and serve as a very effective vortex gate into the sample. The collective mechanism wins over the single-column mechanism at low temperatures. Comparing Eq. (14) with the single-column result we conclude that at high magnetic fields the crossover between the single column and collective regimes is expected at the crossover temperature T_{cr} :

$$T_{cr} \approx \frac{s\varepsilon_0}{8 \ln(1/\pi R^2 n_d)}. \quad (15)$$

For the typical parameters of the compound $\text{Bi}_2\text{Sr}_2\text{CaCu}_2\text{O}_x$ at $n_d = 5 \times 10^{10} \text{ cm}^{-2}$ (corresponding to the matching field of 1 T) and $R = 35 \text{ \AA}$ the crossover is expected at $\approx 20 \text{ K}$.

Our calculations suggest that in the regime of the thermally activated pancake penetration through the surface barrier, the penetration field is roughly 2 times smaller than the penetration field of unirradiated samples at temperatures above the crossover temperature (15) and decreases according to Eq. (14) at lower temperatures. This is consistent with the recent experiment.⁷

We have investigated the influence of columnar defects in layered superconductors on the thermally activated penetration of pancake vortices through the surface barrier. Depending on the position of an isolated column the effective barrier is determined either by vortex hopping from the surface to the column or by detachment of the vortex from the column to the bulk. For a given external field there exists an optimum location of the column for which the barriers for both stages are equal and the reduction of the effective penetration barrier is maximal. The formation of long clusters of columnar defects thrusting the surface offers the most convenient gates for the vortex entry, the effect of cluster-induced depression of the surface barrier decreasing with temperature. Penetration through the clusters always dominates at low temperatures. It would be very interesting to investigate experimentally the temperature dependences of the surface barriers and penetration rates in order to reveal the role of clusters. The proposed mechanism of disorder-assisted surface creep is very general and can be extended to the point disorder containing samples.

ACKNOWLEDGMENTS

We thank C. J. van der Beek, M. Konczykowski, and A. Mel'nikov for helpful discussions. This work was supported by the U.S. DOE, Office of Science, under Contract No. W-31-109-ENG-38.

- ¹C. J. van der Beek, M. Konczykowski, R. J. Drost, P. H. Kes, N. Chikumoto, and S. Bouffard, *Phys. Rev. B* **61**, 4259 (2000).
- ²V. N. Kopylov, A. E. Koshelev, I. F. Schegolev, and T. G. Togonidze, *Physica C* **170**, 291 (1990).
- ³M. Konczykowski, L. Burlachkov, Y. Yeshurun, and F. Holtzberg, *Phys. Rev. B* **43**, 13 707 (1991).
- ⁴R. G. Mints and I. B. Snapiro, *Phys. Rev. B* **47**, 3273 (1993).
- ⁵E. Zeldov, A. I. Larkin, V. B. Geshkenbein, M. Konczykowski, D. Majer, B. Khaykovich, V. M. Vinokur, and H. Shtrikman, *Phys. Rev. Lett.* **73**, 1428 (1994).
- ⁶L. Burlachkov, V. B. Geshkenbein, A. E. Koshelev, A. I. Larkin, and V. M. Vinokur, *Phys. Rev. B* **50**, 16 770 (1994).
- ⁷J. K. Gregory, M. S. James, S. J. Bending, C. J. van der Beek, and M. Konczykowski, preceding paper, *Phys. Rev. B* **64**, 134517 (2001).
- ⁸I. M. Lifshitz and V. Ya. Kirpichenkov, *Zh. Éksp. Teor. Fiz.* **77**, 989 (1979) [*Sov. Phys. JETP* **50**, 499 (1979)].
- ⁹A. I. Buzdin and M. Daumens, *Physica C* **294**, 257 (1998).
- ¹⁰A. Yu. Aladyshkin, A. S. Mel'nikov, I. A. Shereshevsky, and I. D. Tokman, *Physica C* (to be published).
- ¹¹D. Yu. Vodolazov, *Phys. Rev. B* **62**, 8691 (2000).
- ¹²In layered superconductors with very weak interlayer Josephson coupling the image technique gives the energy of the point vortex near the surface with accuracy s/λ . The exact solution and justification of the image approach has been given in A. Buzdin and D. Feinberg, *Phys. Lett. A* **167**, 89 (1992). The exact field distribution for an isolated pancake vortex has been calculated in R. G. Mints, I. B. Snapiro, and E. H. Brandt, *Phys. Rev. B* **54**, 9458 (1996).
- ¹³G. S. Mkrtchyan and V. V. Shmidt, *Sov. Phys. JETP* **34**, 195 (1972); A. Buzdin and D. Feinberg, *Physica C* **235-240**, 2755 (1994); **236**, 303 (1996).
- ¹⁴We remind the reader that in this process a vortex-antivortex pair nucleates at the column; then the *antivortex* leaves the column and hops to the surface, while the *vortex* remains trapped in the column.
- ¹⁵An electrostatic analogy for the problem of vortex interaction with defects has been extensively explored recently in A. Buzdin and M. Daumens, *Physica C* **332**, 108 (2000).
- ¹⁶Note that the column radius R appears in this equation only because our unit of current contains R . In real units this barrier, of course, does not depend on R .
- ¹⁷Because we only have qualitative estimates in this section, we use physical units from the very beginning.